Oecologia
DOI 10.1007/s00442-013-2875-5

PHYSIOLOGICAL ECOLOGY - ORIGINAL RESEARCH

Loss of whole-tree hydraulic conductance during severe drought and multi-year forest die-off

William R. L. Anderegg · Leander D. L. Anderegg · Joseph A. Berry · Christopher B. Field

Received: 30 September 2013 / Accepted: 20 December 2013

Abstract Understanding the pathways through which drought stress kills woody vegetation can improve projections of the impacts of climate change on ecosystems and carbon-cycle feedbacks. Continuous in situ measurements of whole trees during drought and as trees die hold promise to illuminate physiological pathways but are relatively rare. We monitored leaf characteristics, water use efficiency, water potentials, branch hydraulic conductivity, soil moisture, meteorological variables, and sap flux on mature healthy and sudden aspen decline-affected (SAD) trembling aspen (*Populus tremuloides*) ramets over two growing seasons, including a severe summer drought. We calculated daily estimates of whole-ramet hydraulic conductance and modeled whole-ramet assimilation. Healthy ramets experienced rapid declines of whole-ramet conductance during the severe drought, providing an analog for what likely occurred during the previous drought that induced SAD. Even in wetter periods, SAD-affected ramets exhibited fivefold lower whole-ramet hydraulic conductance and sevenfold lower assimilation than counterpart healthy ramets, mediated by changes in leaf area, water use efficiency, and embolism. Extant differences between healthy and SAD ramets reveal that ongoing multi-year forest die-off is primarily driven by loss of whole-ramet hydraulic capability, which in turn limits assimilation capacity. Branch-level measurements largely captured whole-plant hydraulic limitations during drought and mortality, but whole-plant measurements revealed a potential role of other losses in the hydraulic continuum. Our results highlight the importance of a whole-tree perspective in assessing physiological pathways to tree mortality and indicate that the effects of mortality on these forests' assimilation and productivity are larger than expected based on canopy leaf area differences.

Keywords Climate change · Drought · Forest mortality · Sap flux · Water use efficiency · Whole-tree hydraulic conductance

Communicated by Ram Oren.

Electronic supplementary material The online version of this article (doi:10.1007/s00442-013-2875-5) contains supplementary material, which is available to authorized users.

W. R. L. Anderegg (✉)
Department of Ecology and Evolutionary Biology, Princeton University, 106A Guyot Hall, Princeton, NJ 08544-2016, USA
e-mail: anderegg@princeton.edu

L. D. L. Anderegg
Department of Biology, University of Washington, Seattle, WA, USA

J. A. Berry · C. B. Field
Department of Global Ecology, Carnegie Institution for Science, Stanford, CA 94305, USA

Introduction

Global temperatures have increased by about 0.7 °C in the last century, driven in large part by anthropogenic forcing of the climate system (IPCC 2007). Climate change in the twenty first century is likely to bring much higher temperatures and shifts in precipitation patterns, types, and seasonality, and these will impact terrestrial ecosystems (Easterling et al. 2000). Forest ecosystems store nearly half of the carbon found in terrestrial ecosystems (Bonan 2008), and presently serve as a strong and persistent carbon sink (Pan et al. 2011), but climate-related stresses such as drought and fire may compromise the ability of these ecosystems to sequester carbon. Many species appear globally to operate

Published online: 07 January 2014

near their hydraulic limits with relatively minimal hydraulic safety margins and thus could be vulnerable to drought (Choat et al. 2012). Tree mortality is a fundamental process in determining forest ecosystem carbon uptake and storage, and increasing tree mortality rates linked to temperature or drought stress have been observed in tropical (Phillips et al. 2010), temperate (van Mantgem et al. 2009), and boreal ecosystems (Peng et al. 2011). Indeed, widespread forest die-off events have been observed around the globe (Allen et al. 2010). Due to their important role in the earth system, understanding when, where, and how trees die from climate stress is critical for projections of carbon and water cycling with climate change (Anderegg et al. 2012c).

Researchers have suggested a number of mechanisms leading to tree mortality in response to drought and temperature stress (Anderegg et al. 2012a; McDowell et al. 2011; Sala et al. 2012). Our hypothesis is that death is a cascade of multiple failures involving the ability of the plant to respond in a coordinated way to the stress, playing out over multiple years in many species (Anderegg et al. 2012a). While greenhouse manipulations have been used to leverage careful control of climate stresses (e.g., Adams et al. 2009; Galvez et al. 2011; Hartmann et al. 2013) and field manipulation experiments to induce lethal stress on mature trees (e.g., Plaut et al. 2012), detailed in situ physiological measurements of dying trees in a natural setting are relatively rare. Such observations provide an important complement to manipulations because they can identify key physiological processes, particularly phenology and seasonal patterns of repair and recovery, that mediate mortality and incorporate the effects of antecedent conditions.

Given the cross-tissue coordination of water uptake (Sperry 2011), carbon uptake and allocation (Brodribb and Feild 2000; Sala et al. 2012), biotic agent defense (Kane and Kolb 2010), and phloem and xylem transport (Brodribb 2009; Hölttä et al. 2009), a whole-organism perspective may be particularly informative in examining pathways to tree mortality during drought. Most previous research on carbon and hydraulic changes during drought in mature trees has focused on measurements of individual tissues (e.g., Anderegg et al. 2012b; Galiano et al. 2011; but see Plaut et al. 2012). Yet the coordination at an organism scale between gas exchange, hydraulic capacity, and leaf area may be particularly informative in disentangling the processes and feedbacks that mediate tree mortality from drought. Coordination and integration across the entire plant is particularly important when considering the xylem transport system. Because hydraulic vulnerability differs across tissues (Ewers et al. 2000), loss and repair of the hydraulic continuum may not be observed in branch-level measurements (West et al. 2008) and such loss could impair carbohydrate mobilization and transport (Nikinmaa et al. 2013).

We examine here key components of hydraulic performance at a whole-tree scale during ongoing drought-induced forest die-off of trembling aspen (*Populus tremuloides*). As the most widespread tree species in North America, trembling aspen play an important role in ecosystems throughout the Rocky Mountains and Canadian parklands and boreal regions (Perala 1990). Regional aspen mortality, termed sudden aspen decline (SAD), has been documented around the western United States (Anderegg et al. 2012b; Worrall et al. 2008, 2010). Mortality appears to have been induced by a severe drought coupled with elevated temperatures from 2000 to 2003 and has continued through 2012, when another major drought occurred. Aerial survey data from 2008 indicate that SAD has affected roughly 17 % of aspen forests in Colorado (Worrall et al. 2010). Furthermore, this aspen die-off has been shown to lead to substantial biomass loss from forests in Colorado (Huang and Anderegg 2012) and Canada (Michaelian et al. 2011).

Previous research on this multi-year die-off has largely revolved around measurements on single tissues—typically branches—which found substantial hydraulic impairment in SAD branches and roots (Anderegg et al. 2012b), and that hydraulic deterioration in branches builds up over multiple years to cause death long after the inciting drought (Anderegg et al. 2013b). Yet the buildup of hydraulic dysfunction and the dynamics of plant carbon uptake at a whole-ramet level, both during severe drought and during ongoing mortality, are largely unknown. These processes are important for linking tissue-level measurements to whole trees in process-based models (e.g., Fisher et al. 2010; Sperry et al. 1998).

We examine here 2 years, one of which contained a severe drought, of growing season measurements in dying and healthy aspen stands in southwestern Colorado. By examining both the response of healthy ramets to drought stress and the extant differences between healthy and SAD ramets years after the inciting drought, we aim to capture complementary and opposite ends of the mortality process: severe drought similar to the type that induced physiological failures leading eventually to mortality and accumulated physiological damage in SAD trees prior to death. Rather than strict quantification of transpiration and carbon fluxes, we aim to quantify the performance of SAD trees relative to the healthy trees to assess physiological decline during multi-year mortality. We ask: (1) How do whole-ramet changes in canopy evaporative area during severe drought, as captured in leaf characteristics, leaf area, intrinsic water use efficiency, and apparent canopy conductance, affect whole-ramet carbon uptake and hydraulic conductance? (2) How do changes in canopy evaporative area as aspen ramets die affect standing differences in whole-ramet carbon uptake and hydraulic conductance between healthy and

SAD areas? (3) How does whole-ramet hydraulic conductance compare to branch-level hydraulic conductivity and what does this indicate about the relative roles of embolism versus other losses in the hydraulic continuum? (4) Do healthy and dying ramets exhibit similar sensitivities of canopy conductance to vapor pressure deficit as healthy ramets? If the sensitivities are similar, this indicates that the mortality process is consistent with a "sliding down" the stomatal trade-off associated with an optimized carbon cost per unit water observed within and across many species (Oren et al. 1999). If the sensitivities are different, however, mortality may be a fundamental breakdown of this standard relationship (e.g., Katul et al. 2009; Oren et al. 1999), which could yield insight into mortality mechanisms. And (5) are healthy and dying ramets' sensitivities of canopy conductance to VPD related to measured ramet hydraulics?

Materials and methods

Study sites

We examined aspen forests in the San Juan National Forest (37.5°N, 108.3°W) in western Colorado, USA, documented to have experienced some of the most severe SAD in Colorado (Worrall et al. 2008). The San Juan National Forest has an annual mean temperature of 3.2 °C, and receives an average of 500 mm of precipitation annually, 40–60 % of which comes as snow. The region generally experiences snowmelt in mid-late May, a reasonably dry period before the summer monsoons, and a monsoonal precipitation beginning in July and intermittent through leaf senescence in September.

We selected five aspen clones that displayed a gradient of mortality, each clone containing an area with >80 % average crown mortality to an area with <10 % average crown mortality over 100 m, and established a plot at each end of the clone's gradient (henceforth SAD and healthy plots). This gradient of mortality allows comparison of ramets in the process of dying with their visually healthy counterparts in the same clone. Clone boundaries were determined by timing of leaf-out and leaf coloration, described in depth in previous studies (Anderegg et al. 2012b). All study sites were dominant aspen forest with primarily mountain snowberry (*Symphoricarpus oreophilus*) understory and were located between 2,500 and 2,800 m elevation, generally on the lower and drier range of aspen elevation in this forest (Worrall et al. 2008).

Meteorological measurements

We selected one of the five clones to instrument and in which to collect meteorological measurements, as well as continuous measurements of sap flow and soil moisture, during the 2011 and 2012 growing seasons (henceforth Core site). This site was selected for physiological measurements because previous analyses using time-series Landsat imagery to detect SAD indicated that, in 1999, prior to the 2000–2003 drought, both the SAD and healthy areas of the clone were remarkably similar in fraction of non-photosynthetically active vegetation ($NPV_{SAD} = 0.28$; $NPV_{Healthy} = 0.28$) (Huang and Anderegg, in review). NPV has been used successfully to map SAD across this region (Huang and Anderegg 2012) and NPV of the SAD area in 2011 had risen to 0.86, while that of the healthy area remained at 0.31. Thus, both areas of the Core site appear to have been healthy and displayed similar satellite-apparent greenness and NPV prior to the drought, indicating a good site in which to examine SAD since 2000–2003.

We installed temperature sensors (Campbell Scientific CS107), relative humidity sensors (Campbell Scientific CS210), and rain gauges at 2 m height in both the SAD and healthy plots of the Core site. We measured volumetric water content of surface soil (0–30 cm) and deep soil (30–60 cm) using soil moisture probes (Campbell Scientific CS616). Soil became extremely rocky below depths of 60 cm and prevented measurement of deeper moisture. We installed 6–8 soil moisture probes in each plot during each year, allocating ~67 % of probes to surface and ~33 % of probes to deep soil, seeking to capture as much spatial variation as possible within a 8.8-m radius around the plot center. In addition, we installed a net radiometer (Campbell Scientific CNR1) in an exposed area of the SAD stand that was not shaded to measure short-wave, long-wave, and net radiation.

Equipment was installed during June 15–Sept 1, 2011 and May 20–Aug 27, 2012 to capture the vast majority of the growing season in each year. All equipment recorded observations at 5-min intervals and then averaged measurements every half-hour. We checked rain gauges for precipitation at 3- to 7-day intervals, depending on weather forecasts. Due to battery malfunctions in the 2011 growing season, some measurements, particularly in the healthy plot, were only collected intermittently during that growing season.

Sap flow measurements

At the Core site, we installed 30-mm thermal dissipation sap flow sensors in 7–8 mature aspen ramets per treatment in both the SAD and healthy plots. In the SAD plot, sensors were installed in ramets with 20–80 % crown mortality. Two of these ramets in each growing season had 70–80 % crown mortality and were considered "dying" ramets because they died by the end of the growing season (though no SAD-affected ramets have yet been observed to recover,

meaning that all SAD-affected ramet will likely die over the course of several years). However, all calculations presented here average all SAD-affected ramets. The thermal dissipation sensors measure sap flux integrated along their length using the Granier method (Granier and Loustau 1994). Previous research in this forest has indicated that aspen sapwood typically spans 10–30 mm from the outer edge of the bark, and thus this length measures the active sapwood well. Probes were placed on the south or west side of trees, away from any visible scars, after sensitivity tests on three trees in 2011 indicated little difference in flux velocities at different cardinal directions when instrumenting trees with multiple sensors simultaneously. All instrumented trees were thoroughly covered in reflective silver insulation to prevent external thermal gradients that might influence flux measurements. Flux measurements were taken every 5 min and averaged to half-hour intervals.

The Granier method requires setting a zero-flow point, typically based on the maximum temperature difference between probes (ΔT) over a certain period of measurement. We set the zero-flow point at ΔT_{max} over a 24-h period for a given sensor because alternate zero-flow points led to unrealistically high nighttime transpiration. This assumption could lead to underestimation of nocturnal transpiration (Oishi et al. 2008), particularly as only ~50 % of our nights satisfied the two criteria presented by Oishi et al. (2008) of minimum nighttime VPD <0.05 kPa and relatively stable minimum flux for 2 h, and thus we explored this potential by conducting regressions of the zero set-point against minimum nighttime VPD.

To scale sap flux velocities to ramet-level transpiration, we measured sapwood depth at the end of the growing season, by applying methylene blue dye to a tree core and then visually assessing conducting areas. This method has previously been used successfully in aspen (Hogg et al. 1997) and compared well with active uptake of safranin dye in our previous research (Anderegg 2012). Early sensitivity tests on trees outside our plots indicated that sapwood depth did not vary substantially with cardinal direction in near-circular stems, and thus one tree core per ramet was adequate to assess sapwood area. To account for potential biases due to sensors in contact with poorly conductive or non-conductive xylem, we performed corrections with the measured sapwood and heartwood fractions based on equations presented in Clearwater et al. (1999). These corrections were used on 3 of 7 SAD-affected ramets that exhibited sections of non-conducting sapwood in methylene blue dye stains of tree cores.

Leaf area and $\delta^{13}C$ measurements

At all five clones, we assessed leaf area index (LAI) via hemispherical photography in both SAD and healthy plots. Photographs were taken pre-dawn, typically 0500–0600 hours, from plot centers on August 15–16, 2011, and June 6–7, July 5–6, and August 15–16, 2012, with standardized orientation towards north. Photographs were then processed using the Gap Light Analyzer software (Frazer et al. 1999) to calculate LAI with a standard angle of 75° because no plots were on steep (>10°) slopes.

We also collected leaf samples for measurement of bulk leaf $\delta^{13}C$ in each plot of the five stands in August 15–16, 2011. Between 1200–1400 hours, upper canopy leaves were collected via shotgun, severing small twigs with light birdshot. These leaves were immediately placed in sealed plastic bags and then in a dark cooler under ice. The leaves were kept in the dark and under ice until oven-dried at 55 °C within 24 h. Leaves were then ground with a Wiley-mill (30 mesh) and then ground to a powder with a ball-mill. Bulk leaf $\delta^{13}C$ was measured via isotope ratio mass spectronomy (ThermoScientific) and $\delta^{13}C$ in parts per thousand notation (‰) was calculated as $\delta^{13}C = [(\delta^{13}C_{samp}/\delta^{12}C_{samp})/(\delta^{13}C_{ref}/\delta^{12}C_{ref}) - 1] \times 1{,}000$.

Apparent canopy conductance

We calculated the mean apparent canopy stomatal conductance to water vapor (g_c; m s^{-1}) per square meter leaf area for healthy and SAD areas at the Core site using daily maximum stand-level transpiration (E_{max}; kg m^{-2} s^{-1}) and VPD (D; kPa) following the method of Monteith and Unsworth (1990). This approximation takes the form of:

$$g_c = \frac{\gamma \lambda E}{\rho c D}$$

where γ is the psychrometric constant (kPa C^{-1}), λ is the latent heat of vaporization (J kg^{-1}), ρ is the density of moist air (kg m^{-3}), and c is the volumetric heat capacity of moist air at constant pressure (J kg^{-1} C^{-1}). This method requires that D is near the leaf-to-air vapor pressure deficit, that no vertical gradient in D through the canopy exists, and that there is negligible water stored above the measurement of E. Previous studies indicate that these assumptions are typically met in single-canopy aspen forests of similar densities to the forest studied here (Ewers et al. 2005). We then converted g_c values to mmol m^{-2} s^{-1} and examined the decline in canopy conductance as a function of VPD in SAD and healthy ramets using the method presented in Oren et al. (1999), which compares the slope of canopy conductance with ln(VPD) $\{dg_c/d[\ln(\mathrm{VPD})]\}$ against the reference canopy conductance at 1 kPa of VPD (g_{cref}).

Water potentials, leaf size, hydraulic conductivities and $\delta^{13}C$ of leaf sugars

In the Core site, we measured twig water potentials in ramets instrumented with sap flow in both the SAD and

healthy plots during August 15–16, 2011, and June 6–7 and 24–25, July 5–6, and August 15–16, 2012. We made pre-dawn measurements at 0300–0500 hours and midday measurements at 1200–1400 hours. Small distal branch networks, typically 7- to 10-mm basal branch diameter, were collected from mid-canopy with a shotgun. Tall canopies (>10 m) precluded use of ladder and pole-clipper to collect samples. Branch networks were instantly placed in a dark plastic bag for transport. We measured xylem tension with a Scholander-type pressure chamber (PMS Instruments, Corvalis, OR, USA). Small twigs were cut from the distal branch network at least 20 cm and two nodes removed from the initial break for measurement. All samples were measured within 3 min of collection.

From branch networks collected at midday, we randomly selected ~20 leaves per branch for leaf size calculations. We placed flattened leaves on a white surface along with a ruler for length reference, took a digital photograph above the surface, and calculated average leaf size (cm^2) for each ramet during each sampling event using ImageJ software (Schneider et al. 2012).

We collected 2–3 branch segments from each of these branch networks from the midday sampling for determination of hydraulic conductivity (K_s; kg MPa^{-1} m^{-1} s^{-1}). Branch segments of >10 cm length (average diameter of 0.5 cm ± 0.15 cm SD) were cut, instantly misted, and placed in sealed plastic bags (all final segment lengths were >8 cm). Segments were kept hydrated during transport to the laboratory. In the laboratory, segments were re-cut under water with a razor blade and then processed with the standard pressure-flow method (Sperry et al. 1988). Native conductivities were determined, standardized by branch basal area, and segment length.

We also collected leaf samples from these same branch networks for determination of $\delta^{13}C$ of leaf sugars to estimate intrinsic water use efficiency at all four sampling events. From the branches collected during the midday sampling, we excised leaves and instantly placed them in a sealed air-tight plastic bag and in a dark cooler under ice. We took care to make sure that no bags leaked to allow air exchange that might affect isotopic values and placed samples under ice immediately. We followed the same protocol as above in drying and grinding leaves. To extract leaf sugars for isotope analysis, we followed the protocol detailed in Brugnoli et al. (1988). Briefly, dried leaf powder is mixed with PVPP and de-ionized water and centrifuged. The supernatant is collected and filtered through chromatographic columns of resin: DOWEX 1 × 2 to remove positively charged acids and DOWEX 50 W to remove negatively charged acids. The remaining fluid is largely soluble sugars and water, and is thus freeze-dried and weighed for isotopic determination. A recent intercomparison paper found this method adequate for determination of bulk sugar $\delta^{13}C$ (Richter et al. 2009). Isotopic measurements were made via isotope ratio mass spectroscopy at the UC Davis Stable Isotope Facility.

Calculation of whole-plant hydraulic conductance and assimilation

We used established methods to calculate root-to-leaf hydraulic conductance (K_p as opposed to K_s, hydraulic conductivity, which is calculated on branches only) by combining estimates of transpiration from sap flow with water potential differences over a day (Becker et al. 1999; Mencuccini 2003; West et al. 2008; Wullschleger et al. 1998). For each ramet, we calculated the maximum daily transpiration (E; g m^{-2} s^{-1}) rate, which closely aligned with the timing of midday water potential measurements (1200–1400 hours), on a per sapwood area basis across all days for which we had complete sap flow measurements. As in West et al. (2008), we then calculated the difference between midday and pre-dawn xylem tensions as an estimate of the water potential gradient over the course of the day. Whole-plant hydraulic conductance (K_p; g m^{-2} s^{-1} MPa^{-1}) is then calculated as:

$$K_p = \frac{E_{max}}{\left(\Psi_{midday} - \Psi_{predawn}\right)}$$

Growing season water potentials were linearly interpolated between sampling events, which likely underestimates the variation across the summer in water potential. Nonetheless, because this is an assumption, we present in all figures both the directly measured (on sampling dates) and interpolated (between sampling dates) values. We compared the average K_p across all direct-measure sampling dates per ramet with the stomatal canopy conductance estimates generated above.

Due to canopy height and fragility of branches, direct measurement of gas exchange was not possible on mature SAD-affected and healthy ramets. Instead, we used a published model to estimate first-order differences in net assimilation at the whole-ramet scale using a combination of $\delta^{13}C$ of leaf sugars to infer water use efficiency (WUE) averaged over the uptake of those sugars and sap flux to approximate transpiration (Hu et al. 2010). Briefly, this model uses $\delta^{13}C$ of leaf sugars to calculate instantaneous WUE, which can be expressed as the ratio of assimilation (A) to transpiration (E) and also as the difference between atmospheric CO_2 (C_a) concentration and the intracellular CO_2 concentration (C_i) divided by daytime VPD measured in the aspen stand (v) (calculated from 0900 to 1800 hours, as in Hu et al. (2010):

$$\mathrm{WUE} = \frac{A}{E} = \frac{C_a - C_i}{1.6v}$$

The model uses $\delta^{13}C$ of leaf sugars to calculate the isotope discrimination factor (Δ) as:

$$\Delta = \frac{\delta^{13}C_a - \delta^{13}C_{leafsug}}{1 + \delta^{13}C_{leafsug}}$$

For this analysis, $\delta^{13}C$ of the atmosphere was assumed to be −8.5 ‰ measured at Niwot Ridge, CO (Bowling et al. 2005). Then, based on the linear model of Farquhar et al. (1982) which assumes infinite mesophyll conductance, the net assimilation model uses this discrimination factor to calculate C_i necessary for estimating instantaneous WUE:

$$\frac{C_i}{C_a} = \frac{\Delta - a}{b - a}$$

These coefficients are the fractionation caused by the diffusion of CO_2 in air (a; 4 ‰) and the fractionation due to the active site of the enzyme Rubisco (b; 27 ‰). Once C_i has been calculated, it can be used to calculate instantaneous WUE, which we then multiplied by E to derive whole-plant assimilation (Hu et al. 2010).

As in the K_p analysis, we present modeled assimilation values from both the directly measured $\delta^{13}C$ dates (on sampling dates) and temporally interpolated (scaling the average $\delta^{13}C$ of leaf sugars value per treatment across the summer linearly between sampling events) values to ensure that all conclusions are supported by direct measurement periods. Interpolating is a reasonable approach because $\delta^{13}C$ values did not vary extensively across the summer and a previous full Monte Carlo sensitivity analysis using this model indicated that E was responsible for most of the variance in the model, rather than $\delta^{13}C$ (Hu et al. 2010). While recent research has suggested that the linear model of estimating WUE could overestimate instantaneous WUE (Seibt et al. 2008), extensive previous testing with this model indicated little difference between use of the linear model and a more nuanced method (Seibt et al. 2008) that accounts for mesophyll conductance and fractionation due to photorespiration (Hu et al. 2010). Finally, we present whole-plant assimilation values on a per-tree and per-square-meter of ground area (per-tree measurements scaled by stand density for each area) for both healthy and SAD plots to allow comparison between SAD and healthy ramets and regions.

Statistics

Using ramet as the experimental unit to compare between healthy and SAD stems at the Core site, repeated measurements of leaf size, branch hydraulic conductance, xylem tensions, soil moisture, and $\delta^{13}C$ of leaf sugars across multiple sampling periods were analyzed via repeated-measures ANOVA, after checking assumptions of sphericity via Mauchly's Sphericity Test. Differences between the slopes of canopy conductance versus vapor pressure deficit were assessed via ANCOVA. Drawing upon all five clones with paired healthy-SAD plots, we tested differences in leaf area index and $\delta^{13}C$ of bulk leaf tissue across clones via paired t tests, after checking assumptions of normality. All analyses were performed in the R statistical environment (R Core Development Team v.2.12.1).

Results

Meteorology

Meteorological observations confirmed that the study site experienced severe drought during the 2012 growing season. During the 2011 growing season (May–Sept) ember, 16.6 cm of rain fell after a close-to-average winter precipitation (95 % of average total snowpack in snow-water-equivalent). The 2012 growing season, however, had 12.3 cm of growing season rain, well below the long-term (1970–2000) average at this site of 27.9 cm (±8.1 cm SD), after 70 % of average snowpack. Furthermore, the years differed extensively in climatic conditions. In 2011, near-average snowmelt timing (late May) and relatively dispersed rain events throughout the summer led to higher soil moisture values of both surface and deep soil than in 2012 (Fig. 1). By contrast, 2012 had lower overall snowpack, yielded an extremely early snowmelt in late April to early May and had no precipitation until early July (Fig. 1), leading to regional drought status of "Extreme Drought" (PDSI < −4) by July 1 (NOAA NCDC). Datalogger power failures led to gaps in 2011 data, particularly in the healthy treatment, but climatic conditions were recorded consistently in the SAD treatment.

Comparing SAD and healthy areas in the Core site, the healthy plot consistently had higher soil volumetric water content in both years by an average of 0.08 m^3/m^3 for surface soil (repeated-measures ANOVA; $F = 31.7$, $p < 0.00001$) and 0.13 for deep soil (rm-ANOVA; $F = 52.1$, $p < 0.00001$). The SAD plot had consistently higher temperatures 2 m above ground level than the healthy area, although these differences were typically small (<0.5 °C). Where data were available in 2011 and pre-monsoon in 2012, the SAD plot also had higher VPD, though it experienced slightly lower VPD after monsoon in 2012.

Canopy and leaf characteristics

Leaf area index (LAI) measured in five clones via hemispherical photography was consistently lower in SAD plots than in healthy plots (paired t test; $t = 37.6$, $p < 0.00001$) (Fig. 2). Bulk leaf $\delta^{13}C$ values were significantly more enriched in SAD plots than healthy plots as well (paired t

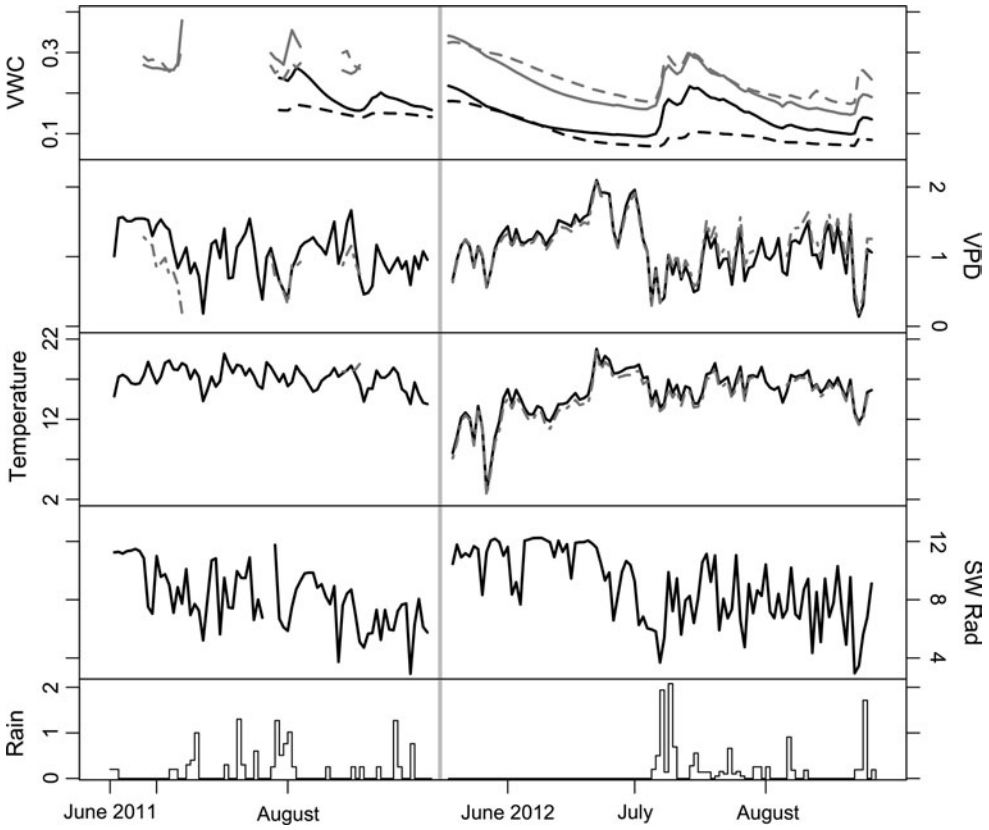

Fig. 1 Meteorological measurements in the Core site over 2011 and 2012 growing seasons of (*bottom* to *top*) rain events (cm), down-welling shortwave radiation (kW m^{-2} day^{-1}), average daily air temperature at 2 m (C), average daily vapor pressure deficit (VPD) at 2 m (kPa), and soil moisture by volumetric water content (VWC) of 0–30 cm surface soil (*solid lines*) and 30–60 cm deep soil (*dashed lines*) (m^3/m^3). *Gray indicates* measurements from the healthy area and *black* from the SAD area

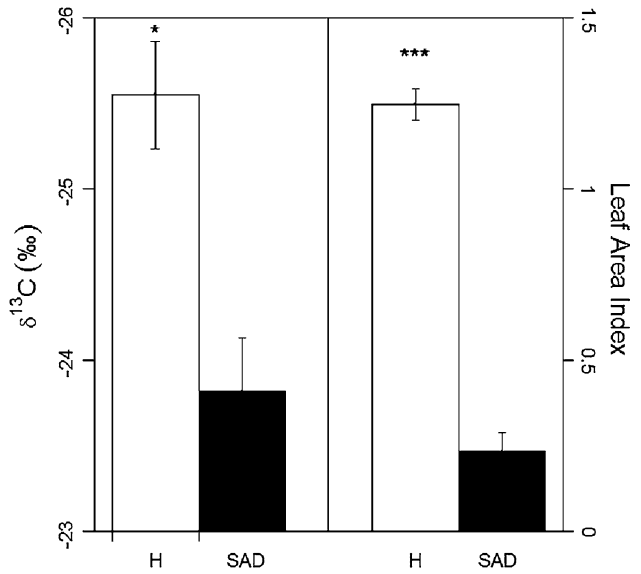

Fig. 2 Enrichment of ^{13}C of bulk leaf tissue (‰) measured in August 2011 and leaf area index of five clones with a healthy (*white*) and SAD (*black*) areas

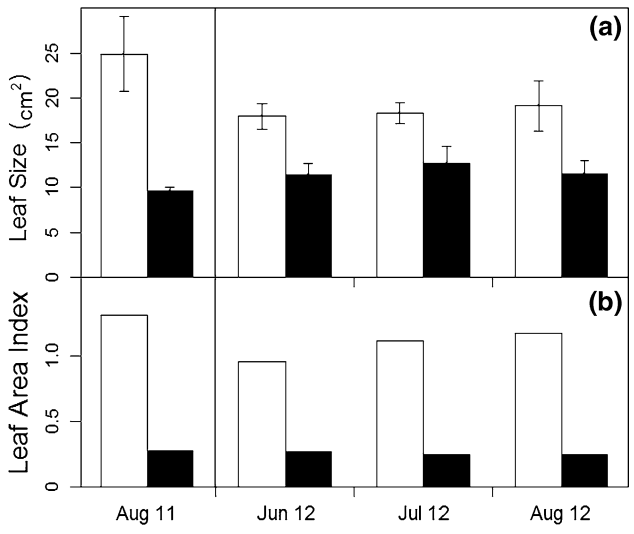

Fig. 3 **a** Average leaf size (cm^2) and **b** leaf area index of ramets in the healthy (*white*) and SAD-affected (*black*) region of the Core site at four sampling events

test; $t = 3.42$, $p = 0.02$) (Fig. 2). Temporal dynamics of leaf size and LAI at the Core site revealed persistent differences between the SAD versus the healthy plot between years and across the growing season (Fig. 3). Average leaf size of healthy ramets was always higher than SAD ramet (repeated-measures ANOVA; $F = 11.4$, $p = 0.007$). Leaf size of healthy ramets was substantially lower in 2012 than in 2011, while it increased slightly in SAD ramets in 2012 compared to 2011. Regarding LAI, the SAD plot exhibited

a constant LAI across the growing season of 2012, but the healthy plot increased LAI through the last sampling in August (Fig. 3). This LAI value of 1.18 in August of 2012 was still lower than the 1.3 measured in August 2011.

Whole-plant versus branch hydraulic conductance

Branch-level measurements of hydraulic conductivity (K_s) revealed temporal changes across a growing season in the healthy plot (repeated-measures ANOVA; $F = 3.8$, $p = 0.04$) and limited response to seasonal variation in the SAD plot (Fig. 4). Nonetheless, healthy K_s was always significantly higher than branch-level SAD K_s (repeated-measures-ANOVA; $F = 14.1$, $p = 0.006$). Low K_s values even in wetter periods (e.g., August 2011) in SAD branches indicated major extant hydraulic impairment in SAD branches.

Clearwater correction for non-functioning sapwood had little effect on sap fluxes used for whole-ramet conductance (correction values of 0.05–0.15 applied on 3 out of 7 trees). Due to gaps in sap flow data in 2011 from datalogger failures, we present primarily 2012 data of whole-ramet conductance (K_p) while including a week of 2011 data for comparison. Whole-plant hydraulic conductance exhibited a roughly similar temporal pattern to branch measurements (Fig. 4). Whole-ramet conductances of SAD ramets were on average 4.9 times (±2.6 SD) lower than healthy ramets (Fig. 4b), and this was due primarily to differences in sap flux (E), rather than water potential (Fig. S1). Interpolated daily measurements of K_p, however, revealed the highly dynamic response of healthy ramet conductance in response to drawdown of soil moisture reserves, particularly evident in the pre-monsoon period up to around July 7, 2012 when healthy ramets' conductances approached SAD levels (Fig. 4b). Healthy ramets' conductances recovered substantially after rain events, while SAD ramets exhibited little post-monsoon increase. Healthy ramets' conductances did reach SAD levels, however, during the second major dry period of the 2012 growing season towards the end of August.

Whole-plant assimilation

Whole-ramet assimilation also differed drastically between SAD and healthy ramets (Fig. 5a). Assimilation differences were larger (23.5-fold ± 8.0 SD) when expressed on a per-square-meter basis (Fig. 5b) due to the low density of surviving ramets in a SAD area, relative to healthy stand density, than when expressed on a per-ramet basis (6.6-fold ± 2.2 SD). Temporal dynamics over the 2012 growing season suggest that the whole-plant assimilation of healthy ramets stayed well above that of SAD ramets until the second major dry-down period (Fig. 5), which experienced around the same soil moisture levels as the pre-monsoon period (Fig. 1).

Canopy conductance versus VPD

Healthy ramets' canopy conductance (g_c) per square meter of leaf area was generally much higher than that of the SAD plot. While both plots exhibited declining conductance with increasing vapor pressure deficit, the slopes of the sensitivity lines differed significantly between healthy and SAD ramets (ANCOVA; $F = 7.4$, $p = 0.04$) (Fig. 6). Healthy ramets had a fairly standard sensitivity to increasing VPD ($m = 0.57$), but SAD ramets exhibited relatively small sensitivity ($m = 0.17$) to increasing VPD. These

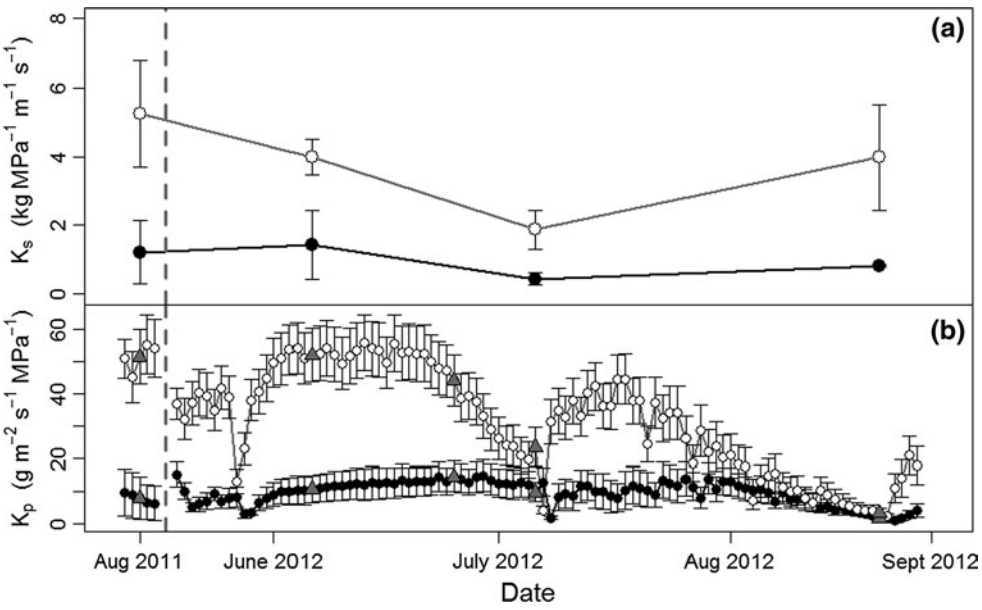

Fig. 4 **a** Branch segment hydraulic conductivity (K_s; mean ± SE; kg MPa^{-1} m^{-1} s^{-1}) and **b** whole-ramet hydraulic conductance (K_p; kg MPa^{-1} day^{-1}) of ramets in the healthy (*white*) and SAD-affected (*black*) region of the Core site. *Gray triangles* represent direct measurements of water potentials

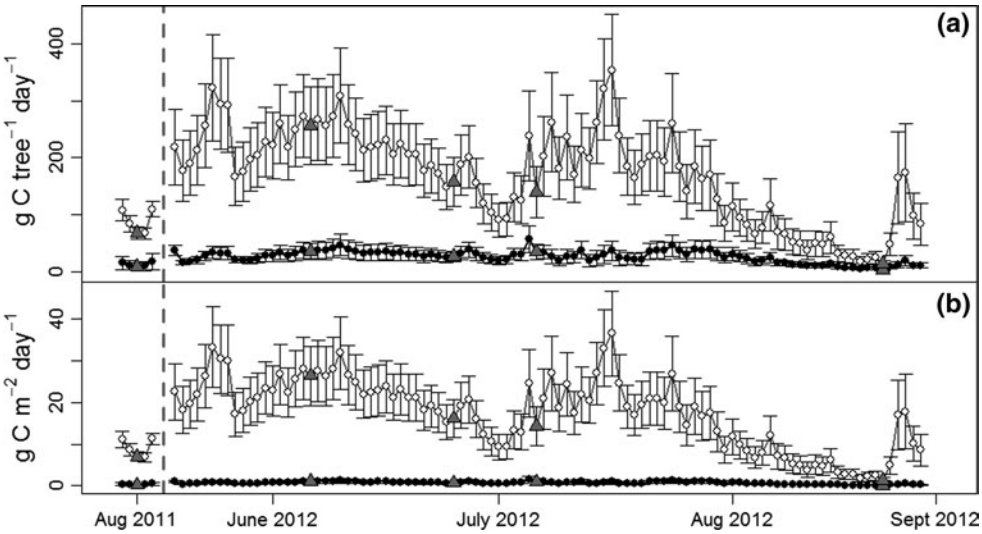

Fig. 5 **a** Average per-tree net assimilation (mean ± SE; grams C tree^{-1} day^{-1}) and **b** per-square-meter of ground net assimilation (mean ± SE; grams C m^{-2} day^{-1}) in the healthy (*white*) and SAD-affected (*black*) region of the Core site. *Gray triangles* represent direct measurements of $\delta^{13}C$ of leaf sugars

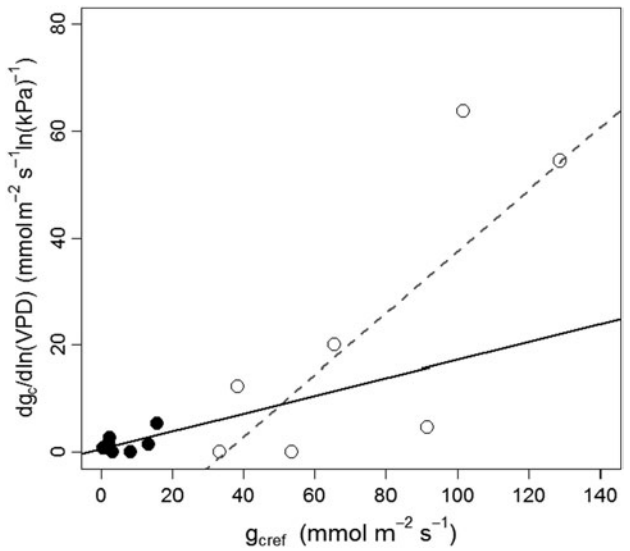

Fig. 6 Reference canopy conductance at 1 kPa (g_{cref}; mmol m^{-2} s^{-1}) versus slope of the sensitivity of canopy conductance to the natural log of vapor pressure deficit [$dg_c/d\ln(VPD)$; mmol m^{-2} s^{-1} ln(kPa)$^{-1}$]. *White circles* indicate healthy ramets (*gray line* is best fit of ordinary least squares regression) and *black circles* indicate SAD ramets (*black line* is best fit of ordinary least squares regression)

differing slopes indicate that SAD ramets are not simply "sliding down" the standard trade-off between maximum canopy conductance at 1 kPa reference VPD and the conductance-versus-VPD slope as described by Oren et al. (1999).

Linking canopy conductance sensitivity to plant hydraulics

Average whole-plant hydraulic conductance was strongly associated with the reference canopy conductance a 1 kPa (g_{cref}) in both healthy ($r^2 = 0.67$; $p = 0.02$) and SAD ramets ($r^2 = 0.92$; $p = 0.0007$) (Fig. 7a). The slope of these relationships, however, differed significantly between healthy and SAD ramets (ANCOVA; $F = 9.64$, $p = 0.03$). Average K_p was not significantly related to the canopy stomatal sensitivity parameter for either healthy ($r^2 = 0.10$; $p = 0.47$) or SAD ($r^2 = 0.11$; $p = 0.46$) ramets (Fig. 7b).

Discussion

We examined whole-ramet water transport and carbon uptake in mature healthy and SAD-affected aspen ramets during a severe drought in western Colorado. Our aim was to characterize whole-ramet responses to drought and standing differences between healthy and SAD-affected ramets in hydraulic and assimilation capability as two ends of the drought-induced mortality process. Given that Ψ_{50} values, the water potential at which 50 % loss of conductivity occurs, for this species in this region tend to fall between −1.0 and −2.3 MPa (Anderegg et al. 2013b; Hacke et al. 2001), midday water potentials of −1.9 to −2.3 MPa in both SAD and healthy ramets during the July and August 2012 sampling events indicated that ramets experienced substantial drought stress during this period (Figure S1).

Canopy evaporative area appeared to play a large role in mediating differences in hydraulic capacity both between SAD and healthy ramets and within the drought in healthy ramets. Leaf size and leaf area index were significantly lower in SAD ramets than healthy ramets (Figs. 2, 3). Differences in average leaf size were larger in 2011 than 2012, driven largely by declines in the healthy ramets' leaf size in 2012, likely due to water stress (Fig. 3). Such transient regulation of leaf area, in particular early leaf-drop in the fall, has also been observed in boreal aspen forests (Barr

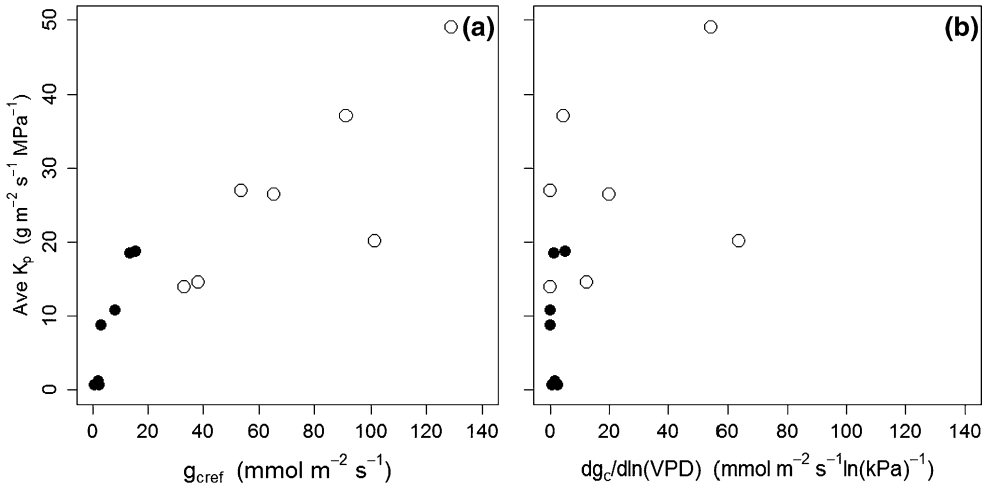

Fig. 7 **a** Average whole-plant hydraulic conductance (g m^{-2} s^{-1} MPa^{-1}) across all 2012 sampling events versus reference canopy conductance at 1 kPa (g_{cref}; mmol m^{-2} s^{-1}) and **b** sensitivity of canopy conductance to the natural log of vapor pressure deficit [dg_c/dln(VPD); mmol m^{-2} s^{-1} ln(kPa)$^{-1}$]. *White circles* indicate healthy ramets and *black circles* indicate SAD ramets

et al. 2007), and appears to play a large role in the interannual differences in carbon fluxes in these forests. Our results indicate that reductions in canopy evaporative area, both in leaf size and LAI, are part of a coordinated set of physiological changes that mediate drought stress from the inciting drought up to mortality.

Both $\delta^{13}C$ of bulk leaf tissue and $\delta^{13}C$ of leaf sugars suggested higher intrinsic water use efficiency in SAD ramets, indicative of stronger stomatal regulation (Fig. 2; Figure S1). Estimated canopy conductance values support that overall the SAD area exhibits much lower conductances to water vapor, but that conductances fall more rapidly in response to VPD in the healthy area (Fig. 6). This aligns well with research documenting that high conductances at low VPD are strongly associated with high stomatal sensitivity to VPD both within and across species (Oren et al. 1999). Strong regulation of canopy conductance, primarily in response to leaf water potential, has been documented in (healthy) boreal aspen forests of differing stand ages (Ewers et al. 2005).

Modeled per-tree assimilation was roughly 6.5 times higher (±2.2 SD) in healthy ramets than in SAD-affected ramets and healthy ramets (Fig. 5). This difference was larger (23.5-fold difference) when considered on a per-ground-area basis, which indicates that the forest carbon uptake of SAD regions is likely to be very low, much lower than what would be expected based on LAI in these areas (Fig. 2). Other studies have documented extensive biomass loss from dead trees in SAD regions averaging 60.3 ± 37.3 Mg/Ha (Huang and Anderegg 2012). Thus, our results suggest that the larger than expected declines in stand assimilation documented here coupled with decomposition of dead trees could influence the carbon balance of these ecosystems, though more detailed simulation of carbon pools is needed to quantify this balance.

Healthy whole-ramet hydraulic conductance (K_p) greatly exceeded that of SAD ramets. We found that K_p largely mirrored branch-level measurements of K_s, but that SAD–healthy K_s disparities were generally less than differences between SAD and healthy ramets' K_p (Fig. 4). Loss of K_s occurred prior to monsoon arrival in the 2012 growing season, yet K_s recovered and K_p declined independently of K_s towards the end of the 2012 growing season (Fig. 4). Thus, declines in K_p pre-monsoon were likely dominated by embolism associated with VPD stress, while K_p declines towards the end of the growing season appear to be dominated by hydraulic dysfunction elsewhere in the hydraulic pathway. Because branch-level measurements reflected whole-tree hydraulic status for much of the period, embolism appears to play a dominant role in whole-plant hydraulic loss. Yet cavitation does not seem to underlie the second decline in K_p, which indicates that in some conditions it may be secondary to other hydraulic losses in the continuum, such as loss of conductivity in the leaf, petiole, roots, or root:soil interface. These other losses in conductivity could be important in mediating some trajectories of drought-induced mortality and warrant further study.

During severe drought, K_p of healthy ramets was quite dynamic over the 2012 growing season, even reaching SAD levels at the two points of maximum water stress (Fig. 4). Given the similar character of the 2012 and 2002 droughts, particularly regarding early snowmelt and a hot and dry early growing season (Anderegg et al. 2013a), the 2012 drought's effects on healthy ramets could potentially be an analog for the 2002 drought that induced sudden aspen decline. We found a ~50 % loss of K_s between June 7

and July 6, 2012 when measured via the standard pressure-flow technique and a ~75 % loss of K_p over the same time. Both K_s and K_p show some recovery following precipitation, yet their loss may still contribute to the accumulated hydraulic deterioration and increased vulnerability found in SAD stands (Anderegg et al. 2013b).

Examining the sensitivity of canopy conductance to VPD, healthy aspen ramets had a stomatal sensitivity-versus-reference conductance slope of 0.57, between the 0.5–0.6 range reported for a wide array of species (Katul et al. 2009), but SAD ramets' slope was dramatically lower (0.17). This considerable departure from the standard relationship indicates that SAD ramets are not simply "sliding down" the curve but in fact have exceptionally low g_{cref} values for a given stomatal sensitivity (Fig. 6). Indeed, apparent canopy conductances in "low conductance" stands in a previous aspen study generally exceeded the apparent conductances documented here in the SAD plot by fourfold (Ewers et al. 2005). This likely indicates that low levels of gas exchange and canopy conductance in SAD ramets are primarily a result of accumulated damage to the plant hydraulic system, rather than strong stomatal control. This is further supported by the relationship between reference canopy conductance and average ramet hydraulic conductance (Fig. 7). Testing for the departure of the slope of this relationship in stressed or dying trees in other species may provide insight into teasing apart the differential constraints on plant transpiration and gas exchange during tree mortality.

Dynamic responses of healthy ramets to severe drought and extant differences between SAD and healthy ramets reveal a suite of coordinated system-level decline across the multiple tissues. This cascade includes declines in canopy evaporative area (Figs. 2, 3) and sapwood area (t test; $t = 2.78$, $p = 0.007$), large declines in carbon uptake and hydraulic capacity (Figs. 4, 5), embolism (Fig. 4), and hydraulically-limited canopy conductances (Fig. 7). These findings underscore that tree death is a systems failure across the whole organism. Previous research indicated that tissue-level hydraulic loss was largely mediated by increased vulnerability to cavitation in SAD stems, along with smaller effects of decreased growth, smaller vessel size, and increased insect attack (Anderegg et al. 2013b). The emergent picture is that death is not simply caused by runaway hydraulic failure but instead by accumulated damage to an aspen tree's water acquisition and transport system via a suite of mechanisms, concurrent with declines in carbon uptake capability, despite no declines of tissue carbohydrate concentrations in SAD-affected ramets (Anderegg et al. 2012b).

As with all methods of scaling individual sensors to tree-level fluxes, some caveats are worth keeping in mind regarding the simulated conductances and assimilation presented here. Rather than detailed quantification of transpiration and carbon fluxes, our primary aim was to assess relative differences between SAD and healthy ramets. First, sap flux measurements were largely assessed at one depth in the sapwood. Changes in flux velocity as a function of depth, which do occur in trembling aspen, would alter the absolute magnitude of sap flow and thus the modeled hydraulic conductance and assimilation. These should not greatly affect differences between SAD and healthy stems, nor the time-course of sap flow over the growing season and with drought, but it nonetheless remains an uncertainty. Second, our selected zero-flow set point for sap flux does not allow for substantial nighttime transpiration or recharge. Regressions of the set point (ΔT_{max}) against minimum nighttime VPD were insignificant ($r^2 = 0.0001$, $p = 0.9$) for healthy, but were significant for SAD-affected ramets ($r^2 = 0.04$, $p = 0.02$). Thus, including nighttime transpiration and recharge could yield higher sap fluxes for SAD-affected ramets, but are unlikely to qualitatively change the differences between healthy and SAD ramets given the order of magnitude differences. Third, inferring WUE from $\delta^{13}C$ of leaf sugars requires the assumption that leaf sugars integrate WUE over several days, depending on turnover of non-structural carbohydrate pools. Thus, the instantaneous (a given day) estimates of WUE and therefore assimilation are not accurate, but previous research suggests that the general time-course (multiple days to weeks) and integrated growing season assimilation from this method are robust (Hu et al. 2010).

We examine here the dynamics of carbon uptake, water loss, and hydraulic conductance in healthy and SAD-affected ramets over two growing seasons. We find consistent and large physiological shifts across a whole ramet both during drought and as ramets approach death. These shifts detail a whole-plant failure of hydraulic capability and assimilation capacity in SAD-affected ramets. Furthermore, they suggest profound decreases in productivity in dying regions that could constitute a climate feedback of tree mortality. Ultimately, in situ and full-tree physiological measurements can inform and guide our understanding and ability to project tree mortality with climate change.

Acknowledgments We thank K. Pham, G. Griffin, M. Anderegg, E. Callaway, C. Kucharczyk, L. Giles and M. Dini for assistance in field and laboratory work, and an anonymous reviewer for helpful comments. Funding for study: NSF DDIG Program. W.R.L.A. was supported in part by an award from the Department of Energy (DOE) Office of Science Graduate Fellowship Program (DOE SCGF) and a NOAA Climate and Global Change Postdoctoral Fellowship.

References

Adams HD et al (2009) Temperature sensitivity of drought-induced tree mortality portends increased regional die-off under global-change-type drought. Proc Natl Acad Sci USA 106:7063–7066

Allen CD et al (2010) A global overview of drought and heat-induced tree mortality reveals emerging climate change risks for forests. For Ecol Manag 259:660–684. doi:10.1016/j.foreco.2009.09.001

Anderegg W (2012) Complex aspen forest carbon and root dynamics during drought. Clim Change 111:983–991

Anderegg WRL, Berry JA, Field CB (2012a) Linking definitions, mechanisms, and modeling of drought-induced tree death. Trends Plant Sci 17:693–700

Anderegg WRL, Berry JA, Smith DD, Sperry JS, Anderegg LDL, Field CB (2012b) The roles of hydraulic and carbon stress in a widespread climate-induced forest die-off. Proc Natl Acad Sci USA 109:233–237

Anderegg WRL, Kane JM, Anderegg LDL (2012c) Consequences of widespread tree mortality triggered by drought and temperature stress. Nat Clim. 3:30–36

Anderegg LDL, Anderegg WRL, Abatzoglou J, Hausladen AM, Berry JA (2013a) Drought characteristics' role in widespread aspen forest mortality across Colorado, USA. Glob Change Biol 19:1526–1537. doi:10.1111/gcb.12146

Anderegg WRL, Plavcová L, Anderegg LDL, Hacke UG, Berry JA, Field CB (2013b) Drought's legacy: multiyear hydraulic deterioration underlies widespread aspen forest die-off and portends increased future risk. Glob Change Biol 19:1188–1196

Barr AG et al (2007) Climatic controls on the carbon and water balances of a boreal aspen forest, 1994–2003. Glob Change Biol 13:561–576

Becker P, Tyree MT, Tsuda M (1999) Hydraulic conductances of angiosperms versus conifers: similar transport sufficiency at the whole-plant level. Tree Physiol 19:445–452

Bonan GB (2008) Forests and climate change: forcings, feedbacks, and the climate benefits of forests. Science 320:1444–1449. doi:10.1126/science.1155121

Bowling DR, Burns SP, Conway TJ, Monson RK, White JWC (2005) Extensive observations of CO_2 carbon isotope content in and above a high-elevation subalpine forest. Glob Biogeochem. Cycles 19:GB3023. doi: 10.1029/2004GB002394

Brodribb TJ (2009) Xylem hydraulic physiology: the functional backbone of terrestrial plant productivity. Plant Sci 177:245–251. doi:10.1016/j.plantsci.2009.06.001

Brodribb TJ, Feild TS (2000) Stem hydraulic supply is linked to leaf photosynthetic capacity: evidence from New Caledonian and Tasmanian rainforests. Plant Cell Environ 23:1381–1388. doi:10.1046/j.1365-3040.2000.00647.x

Brugnoli E, Hubick KT, von Caemmerer S, Wong SC, Farquhar GD (1988) Correlation between the carbon isotope discrimination in leaf starch and sugars of C3 plants and the ratio of intercellular and atmospheric partial pressures of carbon dioxide. Plant Physiol 88:1418–1424. doi:10.1104/pp.88.4.1418

Choat B et al (2012) Global convergence in the vulnerability of forests to drought. Nature 491:752–755

Clearwater MJ, Meinzer FC, Andrade JL, Goldstein G, Holbrook NM (1999) Potential errors in measurement of nonuniform sap flow using heat dissipation probes. Tree Physiol 19:681–687. doi:10.1093/treephys/19.10.681

Easterling DR, Evans JL, Groisman PY, Karl TR, Kunkel KE, Ambenje P (2000) Observed variability and trends in extreme climate events: a brief review. Bull Am Meteorol Soc 81:417–425

Ewers BE, Oren R, Sperry JS (2000) Influence of nutrient versus water supply on hydraulic architecture and water balance in *Pinus taeda*. Plant Cell Environ 23:1055–1066

Ewers BE, Gower ST, Bond-Lamberty B, Wang CK (2005) Effects of stand age and tree species on canopy transpiration and average stomatal conductance of boreal forests. Plant Cell Environ 28:660–678. doi:10.1111/j.1365-3040.2005.01312.x

Farquhar G, O'Leary M, Berry J (1982) On the relationship between carbon isotope discrimination and the intercellular carbon dioxide concentration in leaves. Aust J Plant Physiol 9:121–137

Fisher R et al (2010) Assessing uncertainties in a second-generation dynamic vegetation model caused by ecological scale limitations. New Phytol 187:666–681

Frazer GW, Canham CD, Lertzman KP(1999) Gap Light Analyzer (GLA), Version 2.0:Imaging software to extract canopy structureand gap light transmission indices from true-colour fisheye photographs, users manual andprogram documentation. Simon Fraser University, Burnaby

Galiano L, Martínez-Vilalta J, Lloret F (2011) Carbon reserves and canopy defoliation determine the recovery of Scots pine 4 yr after a drought episode. New Phytol 190:750–759

Galvez DA, Landhäusser SM, Tyree MT (2011) Root carbon reserve dynamics in aspen seedlings: does simulated drought induce reserve limitation? Tree Physiol 31:250–257. doi:10.1093/treephys/tpr012

Granier A, Loustau D (1994) Measring and modeling the transpiration of a maritime pine canopu from sap-flow data. Agric For Meteorol 71:61–81

Hacke UG, Stiller V, Sperry JS, Pittermann J, McCulloh KA (2001) Cavitation fatigue. Embolism and refilling cycles can weaken the cavitation resistance of xylem. Plant Physiol 125:779–786

Hartmann H, Ziegler W, Trumbore S (2013) Lethal drought leads to reduction in nonstructural carbohydrates in Norway spruce tree roots but not in the canopy. Funct Ecol 27:413–427. doi:10.1111/1365-2435.12046

Hogg EH et al (1997) A comparison of sap flow and eddy fluxes of water vapor from a boreal deciduous forest. J Geophys Res Atmos 102:28929–28937

Hölttä T, Mencuccini M, Nikinmaa E (2009) Linking phloem function to structure: analysis with a coupled xylem–phloem transport model. J Theor Biol 259:325–337. doi:10.1016/j.jtbi.2009.03.039

Hu J, Moore DJP, Riveros-Iregui DA, Burns SP, Monson RK (2010) Modeling whole-tree carbon assimilation rate using observed transpiration rates and needle sugar carbon isotope ratios. New Phytol 185:1000–1015. doi:10.1111/j.1469-8137.2009.03154.x

Huang C-Y, Anderegg WRL (2012) Large drought-induced aboveground live biomass losses in southern Rocky Mountain aspen forests. Glob Change Biol 18:1016–1027

IPCC (2007) Contribution of Working Groups I, II and III to the Fourth Assessment Report of the Intergovernmental Panel on Climate Change.IPCC, Geneva

Kane J, Kolb T (2010) Importance of resin ducts in reducing ponderosa pine mortality from bark beetle attack. Oecologia 164:601–609. doi:10.1007/s00442-010-1683-4

Katul GG, Palmroth S, Oren RAM (2009) Leaf stomatal responses to vapour pressure deficit under current and CO2-enriched atmosphere explained by the economics of gas exchange. Plant Cell Environ 32:968–979

McDowell NG, Beerling DJ, Breshears DD, Fisher RA, Raffa KF, Stitt M (2011) The interdependence of mechanisms underlying climate-driven vegetation mortality. Trends Ecol Evol 26:523–532. doi:10.1016/j.tree.2011.06.003

Mencuccini M (2003) The ecological significance of long-distance water transport: short-term regulation, long-term acclimation and the hydraulic costs of stature across plant life forms. Plant Cell Environ 26:163–182. doi:10.1046/j.1365-3040.2003.00991.x

Michaelian M, Hogg EH, Hall RJ, Arsenault E (2011) Massive mortality of aspen following severe drought along the southern edge of the Canadian boreal forest. Glob Change Biol 17:2084–2094. doi:10.1111/j.1365-2486.2010.02357.x

Nikinmaa E et al (2013) Assimilate transport in phloem sets conditions for leaf gas exchange. Plant Cell Environ 36:655–669. doi:10.1111/pce.12004

Oishi AC, Oren R, Stoy PC (2008) Estimating components of forest evapotranspiration: a footprint approach for scaling sap flux measurements. Agric For Meteorol 148:1719–1732

Oren R et al (1999) Survey and synthesis of intra- and interspecific variation in stomatal sensitivity to vapour pressure deficit. Plant Cell Environ 22:1515–1526

Pan Y et al (2011) A large and persistent carbon sink in the world's forests. Science 333:988–993. doi:10.1126/science.1201609

Peng C et al (2011) A drought-induced pervasive increase in tree mortality across Canada's boreal forests. Nat Clim Change 1:467–471

Perala DA (1990)*Populus tremuloides* Michx.Quaking aspen. In: Burns RM, Honkala BH (eds).Silvics of North America, vol 2:Hardwoods. USDA Forest Service Agricultural Handbook654. US Forest Service, Washington, DC, pp 555–569

Phillips OL et al (2010) Drought-mortality relationships for tropical forests. New Phytol 187:631–646. doi:10.1111/j.1469-8137.2010.03359.x

Plaut JA et al (2012) Hydraulic limits preceding mortality in a piñon–juniper woodland under experimental drought. Plant Cell Environ 35:1601–1617

Richter A et al (2009) Preparation of starch and soluble sugars of plant material for the analysis of carbon isotope composition: a comparison of methods. Rapid Commun Mass Spectrom 23:2476–2488. doi:10.1002/rcm.4088

Sala A, Woodruff DR, Meinzer FC (2012) Carbon dynamics in trees: feast or famine? Tree Physiol. doi: 10.1093/treephys/tpr143

Schneider CA, Rasband WS, Eliceiri KW (2012) NIH Image to ImageJ: 25 years of image analysis. Nat Meth 9:671–675

Seibt U, Rajabi A, Griffiths H, Berry JA (2008) Carbon isotopes and water use efficiency: sense and sensitivity. Oecologia (Berlin) 155:441–454. doi:10.1007/s00442-007-0932-7

Sperry JS (2011) Hydraulics of vascular water transport mechanical integration of plant cells and plants, vol 9. In: Wojtaszek P (ed) Signalling and communication in plants: mechanical integration of plant cells and plants. Springer, Heidelberg, pp 303–327

Sperry JS, Donnelly JR, Tyree MT (1988) A method for measuring hydraulic conductivity and embolism in xylem. Plant Cell Environ 11:35–40. doi:10.1111/j.1365-3040.1988.tb01774.x

Sperry JS, Adler FR, Campbell GS, Comstock JP (1998) Limitation of plant water use by rhizosphere and xylem conductance: results from a model. Plant Cell Environ 21:347–359. doi:10.1046/j.1365-3040.1998.00287.x

van Mantgem PJ et al (2009) Widespread increase of tree mortality rates in the western United States. Science 323:521–524. doi:10.1126/science.1165000

West AG, Hultine KR, Sperry JS, Bush SE, Ehleringer JR (2008) Transpiration and hydraulic strategies in a piñon-juniper woodland. Ecol Appl 18:911–927

Worrall JJ et al (2008) Rapid mortality of *Populus tremuloides* in southwestern Colorado, USA. For Ecol Manag 255:686–696. doi:10.1016/j.foreco.2007.09.071

Worrall JJ, Marchetti SB, Egeland L, Mask RA, Eager T, Howell B (2010) Effects and etiology of sudden aspen decline in southwestern Colorado, USA. For Ecol Manag 260:638–648. doi::10.1016/j.foreco.2010.05.020

Wullschleger SD, Meinzer FC, Vertessy RA (1998) A review of whole-plant water use studies in tree. Tree Physiol 18:499–512. doi:10.1093/treephys/18.8-9.499

Monteith JL, Unsworth M (1990) Principles of environmental physics. Butterworth-Heinemann, Woburn